



HAL
open science

Viscosity of carbon nanotubes water based nanofluids: Influence of concentration and temperature

Salma Halelfadl, Patrice Estellé, Bahadir Aladag, Nimeti Doner, Thierry Maré

► To cite this version:

Salma Halelfadl, Patrice Estellé, Bahadir Aladag, Nimeti Doner, Thierry Maré. Viscosity of carbon nanotubes water based nanofluids: Influence of concentration and temperature. *International Journal of Thermal Sciences*, 2013, 71, pp.111-117. 10.1016/j.ijthermalsci.2013.04.013 . hal-00821792

HAL Id: hal-00821792

<https://hal.science/hal-00821792>

Submitted on 13 May 2013

HAL is a multi-disciplinary open access archive for the deposit and dissemination of scientific research documents, whether they are published or not. The documents may come from teaching and research institutions in France or abroad, or from public or private research centers.

L'archive ouverte pluridisciplinaire **HAL**, est destinée au dépôt et à la diffusion de documents scientifiques de niveau recherche, publiés ou non, émanant des établissements d'enseignement et de recherche français ou étrangers, des laboratoires publics ou privés.

1 **Viscosity of carbon nanotubes water based nanofluids: Influence of**
2 **concentration and temperature**

3 **Salma Halelfadl ^a, Patrice Estellé ^{b,*}, Bahadir Aladag ^c,**
4 **Nimeti Doner ^c, Thierry Maré ^a**

5
6 ^a UEB, LGCGM EA3913, Equipe Matériaux et Thermo-Rhéologie, Université Rennes 1, IUT
7 de Rennes, 3 rue du Clos Courtel, BP 90422, 35704 Rennes Cedex 7, France

8
9 ^b UEB, LGCGM EA3913, Equipe Matériaux et Thermo-Rhéologie, Université Rennes 1, IUT
10 de Saint-Malo, Rue de la Croix Désilles, CS51713, 35417 Saint-Malo Cedex, France

11
12 ^c Department of Mechanical Engineering, Dumlupinar University, 43270 Kutahya, Turkey

13
14
15 * Author to whom correspondence should be addressed.

16 Electronic mail: patrice.estelle@univ-rennes1.fr
17 IUT de Rennes, 3 rue du Clos Courtel, BP 90422,

18 35704 Rennes Cedex 7, France

19 Tel: +33 (0) 23 23 42 00

20 Fax: +33 (0) 2 23 23 40 51

21
22 **Abstract:**

23
24 Experimental results on the steady state viscosity of carbon nanotubes water-based nanofluids
25 are presented considering the influence of particle volume fraction and temperature ranging
26 from 0 to 40°C. The suspensions consist of multi-walled carbon nanotubes dispersed in de-
27 ionized water and they are stabilized by a surfactant. The aspect ratio of nanotubes is close to
28 160 and the particle volume fraction varies between 0.0055% and 0.55%. It is shown that the
29 nanofluids behave as shear-thinning materials for high particle content. For lower particle
30 content, the nanofluids are quite Newtonian. It is also observed that the relative viscosity of
31 nanofluids at high shear rate does not vary with temperature. Moreover, the evolution of
32 relative viscosity at high shear rate is well predicted by the Maron-Pierce model considering
33 the effect of nanoparticles agglomerates.

34
35
36
37 **Keywords: viscosity, CNT nanofluid, shear-thinning, agglomerates, temperature**
38
39
40

41
42
43
44
45
46
47
48
49
50
51
52
53
54
55
56
57
58
59
60
61
62
63
64
65
66
67
68
69
70
71
72
73
74
75

Nomenclature

- L length of nanotubes
- d average diameter of nanotubes
- r aspect ratio of nanotube, with $r = L/d$
- μ_{bf} viscosity of base fluid
- μ_{nf} viscosity of nanofluid
- η intrinsic viscosity
- μ_r relative viscosity
- ϕ nanoparticle volume fraction
- ϕ_m maximum packing volume fraction
- ϕ_a effective volume fraction of aggregates
- a radius of nanoparticles
- a_a effective radii of aggregates
- D fractal index

1. Introduction

Nanofluids are colloidal suspensions containing nanometer-sized particles of metals, oxides, carbides, nitrides, or nanotubes dispersed in a base fluid. The base fluid is usually a conventional fluid such as water, glycol, ethylene glycol, engine oil, etc. Over the past decade, nanofluids have attracted much interest owing to their high thermal conductivity and thermal performance compared to base fluids [1-6]. The thermal enhancement effects and the viscosity of nanofluids are strongly dependent on particle size and concentration, the nature of the base fluid, temperature and the presence of nanoclusters.

From a practical point of view, the viscosity of nanofluids is an important property for applications involving fluid flow and it is used to calculate the required pumping power. The viscosity can change due to the addition of solid nanoparticles and can cause the increase of pressure drops, affecting the efficiency of energy systems. It is also closely related to the stability and the structure of solid nanoparticles. The nanoparticle can agglomerate even at low concentration and also in the presence of a surfactant. In addition, it is well established that the shear-thinning behavior of nanofluids is mainly associated with the shape of nanoparticles and it is enhanced with the presence of nanoparticles agglomerates [7-11].

76 Carbon nanotubes (CNTs) nanofluids have attracted much attention because of their
77 remarkable properties. Indeed, it was proved that carbon nanotubes nanofluids have a high
78 thermal conductivity, high electrical conductivity [12,13] and efficient mechanical properties
79 [14]. The preliminary efforts were to treat and modify the surface of the CNTs to improve
80 their solubility and to investigate the effect of surfactant and methods to disperse the
81 nanotubes [15-18]. Nasiri et al. [18] have shown that the CNT structure and stability are
82 strongly dependant on the functionalization and preparation methods of the nanosuspensions.
83 The effect of chitosan as a dispersing agent on the viscosity of multi-wall carbon nanotubes
84 (MWCNTs) dispersed in water was investigated by Phuoc et al. [19]. They showed that the
85 rheological behavior of nanofluids is affected by both the quantity of chitosan and the CNT
86 particle content.

87 Garg et al. [20] studied the effect of dispersing energy (ultra-sonication) on the viscosity of
88 MWCNT aqueous-based nanofluids. They showed that these nanofluids exhibit a shear
89 thinning behavior which is not related to the presence of the surfactant used. They have also
90 shown that sonication time is first associated with declustering of nanoclusters CNT
91 nanofluid. Then, increasing the sonication time breaks the nanotubes leading to less marked
92 shear-thinning behavior of the nanofluid because of the shorter sizes of the nanotubes. Yang
93 et al. [21] have also shown the effects of frequency and time of ultrasonication on
94 agglomerate size and aspect ratio of nanotubes dispersed in oil. They reported that the aspect
95 ratio of the nanotubes decreases both the dispersing time and the energy increase, resulting in
96 less viscous nanosuspensions. The shear-thinning behavior of CNT nanofluids was also
97 observed by Kanagaraj et al. [22]. They have investigated the rheological behavior of CNT
98 nanofluid under a CNT weight fraction of 1% and for a temperature range of 20 °C to 50°C
99 and shear rate ranging from 0 to 1000s⁻¹. Rheological study of Ponmozhi et al [23] has also
100 demonstrated the shear-thinning behavior of CNT water-based nanofluids and the viscosity
101 rise with CNT volume concentration at fixed shear rate and temperature. It was also shown
102 that CNT water-based nanofluids can behave as a shear time dependent material due to the
103 time dependency of agglomeration and disagglomeration kinetics under shear, which is linked
104 to the structural network of the nanofluids [24]. Hence, the rheological behavior of CNT
105 nanofluids can evolve following its preshear history [25]. The effects of base fluid and
106 concentration on the rheological behavior of MWCNTs were investigated by Chen et al. [26].
107 They observed a Newtonian behavior for the studied MWCNTs dispersed in silicone oil,
108 glycerol or water for all concentrations and temperatures. They also reported the effect of
109 temperature; the viscosity of nanofluids decreases when the temperature increases.

110 As far as we know, there are few reports of the rheological properties of aqueous CNT
111 nanofluids. To date, no attempts have been made to interpret the rheological data of such
112 nanofluids with the presence of particle agglomerates. With this goal, the present paper
113 reports an experimental investigation of the rheological properties of CNT water-based
114 nanofluids stabilized by SDBS as surfactant. Here we focus our study on the influence of
115 particle concentration and temperature. In the first part, we present the CNT water-based
116 nanofluids used in the study. The experiments for rheological measurements are then detailed
117 in section 3. In section 4, experimental results are presented and discussed in terms of the
118 influence of particle content and temperature on the viscosity of CNT suspensions. We
119 examine various theoretical viscosity models to predict the relative viscosity of CNT
120 nanofluids at high shear rate and show that it is well represented by the modified Maron-
121 Pierce equation considering the influence of nanoparticles agglomerates.

122

123 **2. Materials**

124

125 **2.1 Nanofluid**

126

127 A CNT water-based suspension was provided by Nanocyl (Belgium). According to Nanocyl's
128 specification, this suspension consists of MWCNTs (carbon purity 90%) dispersed in a base
129 fluid of de-ionized water and surfactant from ultrasonication, and was stable for several
130 months. The dimensions of the nanotubes are 1.5 μm in average length L and 9.2 nm in
131 average diameter d respectively. This leads to an average aspect ratio $r=L/d\approx 163$. The density
132 of the nanotubes is 1800 kg/m^3 . The weight fraction of nanotubes is 1%. This corresponds to a
133 volume fraction of 0.55%. The surfactant used is sodium dodecyl benzene sulfonate (SDBS).
134 The quantity of surfactant represents 2% of the total weight of the nanosuspension. As it is
135 well known that carbon nanotubes have a hydrophobic surface, the surfactant is used to
136 disperse and stabilize the particles and reduce the presence of aggregates [15]. The base fluid
137 was also independently prepared and provided by Nanocyl.

138

139 **2.2 Suspensions preparation**

140 The suspension provided by Nanocyl was used as a starting material to prepare suspensions
141 with various lower mass concentrations of 0.75, 0.5, 0.2, 0.1, 0.05 and 0.01%. This
142 corresponds to a volume fraction of 0.418, 0.278, 0.111, 0.055, 0.027 and 0.00555%
143 respectively. De-ionized water was used to dilute and prepare these suspensions. The
144 appropriate mass of water was precisely measured and then introduced in the initial

145 suspension to reach the required mass (or volume) fraction in nanotubes. The mixture was
146 stirred with a mixer for 30min and then remained at rest. The 30min stirring of each
147 suspension was repeated 24hours later. Mechanical stirring is used to ensure uniform
148 dispersion of nanoparticles and prevent initial agglomeration of nanoparticles in the base
149 fluid. Thereafter, all the suspensions were stored in a container at ambient temperature. No
150 observable sedimentation was noticed before rheological measurements. Following the same
151 procedure, the initial base fluid was also diluted to obtain the base fluids corresponding to the
152 different nanofluids previously prepared. The volume fraction of both tested nanofluids and
153 corresponding base fluids are reported in Table 1.

154

155 **3. Experiments**

156 **3.1 Characterization of nanofluids**

157 Scanning Electron Microscopy (SEM) characterization of the starting nanofluid suspension
158 was preliminary performed to investigate the dispersion state of the nanoparticles within the
159 base fluid, and evaluate the presence and the size of the aggregates [25]. As reported in Figure
160 1, it is shown that the nanotubes are entangled and the starting nanofluid suspension is mainly
161 in the form of aggregates with a maximal aggregate size about 4 times higher than the average
162 length of the nanotubes.

163

164

165 **3.2 Rheological measurements**

166

167 Rheological measurements of nanofluid samples were performed using a stress controlled
168 rheometer (Malvern Kinexus Pro) in a cone and plate configuration under controlled
169 temperature. The temperature was controlled using a Peltier temperature control device
170 located below the lower plate. Thermal clovers were also used to ensure constant temperature
171 within the sample gap. For all experiments, the cone diameter was 60mm and the cone angle
172 was 1°.

173 The working temperature was varied from 0°C to 40°C with an interval of 10°C. The higher
174 temperature was limited to 40°C because the surfactant addition in nanosuspensions limits
175 applications at high temperatures [5,6]. It has been shown that above 60°C the bonding
176 between surfactant and nanoparticles can be damaged [2,4]. The nanofluid will also lose its
177 stability and sedimentation of nanoparticles will occur [3]. For example, SDBS was observed
178 to fail at elevated temperatures in [1]. This was also observed from our experiments at 50°C,
179 as the measured shear viscosity, which varies from one stress to another, indicates the

180 unstable structure under shear (not reported here). The limitation of high temperature was also
181 used to prevent water evaporation from the sample due to the duration of the rheological
182 experiments.

183 Each tested volume sample was taken from its container with a syringe-type automatic pipette
184 and transferred to the lower plate, taking care that no air bubbles were entrapped in the
185 sample. Hence, the cone is displaced to achieve the required sample gap. The excess of
186 sample was eventually removed. The sample was allowed to equilibrate for 5 min before
187 starting the experiment. It should be mentioned that a new sample was used for each
188 measurement and that both cone and plate were cleaned between each measurement.
189 Moreover, no high mixing or sonification was applied to the nanofluids before taking it for
190 rheological measurement. Therefore, no preshear was applied to the samples before testing
191 them. As a consequence, it is considered that each sample has been subjected to the same
192 shear history before being tested. Actually, rheological properties of CNT nanofluids are
193 sensitive to preshear history effect [25].

194 Stress-controlled measurements were performed by imposing a logarithmic stress ramp under
195 steady-state conditions with maximum step duration of 180s. Once a steady-state flow was
196 achieved and maintained for 10s, the shear rate was measured. The applicability of the shear
197 stress range was subject to a preliminary evaluation to ensure steady-state flow at low shear
198 stress, and to avoid flow instability and sample ejection at high shear stress, in particular for
199 suspensions with lower mass content in particles. The end value of the shear stress ramp may
200 vary following the tested suspension, and was set in order to reach a shear rate of 1000s^{-1} for
201 each nanosuspension. The experiments were also repeated at least once to both verify the
202 repeatability of the shear viscosity measurement and the suspension stability with time.

203 Following the same experimental procedure, another series of experiments were conducted to
204 evaluate the rheological behavior of the base fluids corresponding to the nanofluids with
205 different volume fraction. The torque resolution of the rheometer is 0.1 nNm. This means that
206 the uncertainty of shear stress with the cone and plate geometry used is $1.7 \cdot 10^{-3}$ Pa. The
207 angular velocity resolution is at least 10 nrad/s. The uncertainty of shear rate, which only
208 depends on angular velocity and cone angle, is less than $5.73 \cdot 10^{-7} \text{ s}^{-1}$. This leads to an
209 uncertainty in apparent viscosity less than 4% within the shear rate range investigated.

210

211 **4. Results and discussion**

212

213 **4.1 Viscosity measurement validation and viscosity of base fluids**

214 To evaluate the rheometer uncertainty and the experimental procedure, distilled water was
215 tested at 20°C following the procedure described here before and for two replicates. As
216 expected, distilled water exhibits a Newtonian behavior within the shear rate range
217 investigated. The viscosity value of distilled water was 1.0345, which closely matches with its
218 theoretical values at 20°C. The relative deviation is less than 3.5%. This is of the same order
219 of magnitude as the experimental uncertainty.

220 Figure 2 reports the shear viscosity of the base fluid for the starting nanofluid at 0.55% in
221 volume concentration of nanoparticles. It is observed from figure 2 that this base fluid
222 behaves in Newtonian manner, as the apparent viscosity is constant within the shear rate range
223 investigated. The shear viscosity value of this base fluid at 20°C is 1.129mPa.s. This is higher
224 than the viscosity of de-ionized water, showing the influence of SDBS. It is also shown from
225 figure 1 that the viscosity of the base fluid decreases when the temperature is increased.

226 The shear viscosity of the base fluid of the nanofluid at 0.0055% in volume fraction of
227 nanoparticles is reported in figure 3. We observe than this base fluid is also Newtonian as the
228 shear viscosity is constant within the shear rate range investigated and its viscosity is very
229 close to the one of de-ionized water. A similar effect of temperature increase is also obtained
230 for the viscosity of this base fluid. Too, a Newtonian behavior for all tested base fluids is thus
231 observed.

232 In Table 1, the shear viscosities of all base fluids (corresponding to all tested nanofluids) are
233 given as a function of volume fraction in SDBS. Table 1 shows that, for all the tested
234 temperatures, the shear viscosity of base fluids slowly decreases with the decrease of SDBS
235 volume fraction. This can be explained by the dilution of the base fluids and the reduction of
236 the presence of SDBS. When the volume fraction of SDBS is lower than 0.169%, the shear
237 viscosity of the base fluid is quite constant and tends to the viscosity of water. As reported
238 before, when the temperature increases, the shear viscosity of the base fluids decreases.

239

240 **4.2 Viscosity of nanofluids: Influence of concentration and temperature**

241 Figure 4 reports the evolution of the shear viscosity depending on shear rate for CNT
242 nanofluid at 0.278% in volume fraction and for all the tested temperatures. Figure 4 shows
243 that the nanofluid behaves as a shear-thinning fluid as the shear viscosity decreases when the
244 shear rate increases. The good agreement between two replicates of rheological measurement
245 for this nanofluid at 10°C can also be noted in figure 4. This shows the repeatability of the
246 measurement and the stability of the nanofluid. Similar trends were obtained for all nanofluids
247 and temperatures.

248 In figure 5, the shear viscosity of CNT nanofluid at 0.0055% in volume fraction is plotted
249 against shear rate. Comparison of figure 4 and 5 shows that the rheological behavior of
250 nanofluids is strongly dependent on the volume fraction of nanotubes within the nanofluids.
251 This trend can also be shown by figure 6, when we compare the shear viscosity of all
252 nanofluids at 20°C. In figure 6 we observe that the higher the concentration, the higher the
253 shear-thinning behavior and the extent of the shear-thinning region. The transition between
254 shear-thinning behavior and Newtonian behavior of the nanofluids is for a volume fraction of
255 0.055%. Figure 5 also shows that the shear viscosity increases with CNT concentration for a
256 given shear rate. It should be noted that the nanofluid with lower concentration have lower
257 shear viscosity than that of the base fluid. This effect is probably due to the lubricative effect of
258 nanoparticles [26].

259 It is shown from figures 4 and 5 that temperature has a strong effect on the rheological
260 properties of CNT nanofluids. Actually, the nanofluids viscosity decreases with increasing
261 temperature, as generally reported for a wide class of nanofluids and previously observed for
262 the base fluids.

263 As reported in the literature, the shear-thinning effect, in addition to the effect of nanotubes
264 length, can be attributed to the disagglomeration of the nanotube clusters and the alignment of
265 the agglomerates and nanotubes during shear, resulting in less viscous force.

266 It can be noted that the shear-thinning behavior of the studied CNT nanofluids is stronger than
267 the one reported by Kanagaraj et al. [22], which indicates a great effect of the aspect ratio and
268 the agglomerates network of the nanotubes on the shear viscosity. In the present work, the
269 aspect ratio of the nanotubes is higher than the aspect ratio ($r = L/d \approx 8$) of the nanoparticles
270 used in [22]. Our results are also consistent with the work of Ding et al. [27], which showed
271 the shear-thinning behavior of aqueous suspension of carbon nanotubes at 20 and 40°C within
272 the shear rate range 1 to 1000s^{-1} . Shear-thinning of MWCNT-based aqueous nanofluids was
273 also observed by Garg et al. [20] at 15 and 30°C for low shear rate range between 0 and 80 s^{-1}
274 and by Maré et al. [28] for temperatures ranging from 0°C to 10°C.

275 Figure 7 reports the relative viscosity at a high shear rate of 1000s^{-1} , defined as the ratio of the
276 CNT nanofluid viscosity at high shear rate to the viscosity of the base fluid at the same shear
277 rate, as a function of all tested temperatures. While nanofluids and base fluids are strongly
278 dependent on temperature, it is also observed from figure 7 that the relative viscosity is quite
279 constant for the tested temperatures under the experimental uncertainty. The relative viscosity
280 of nanofluids at a high shear rate in function of nanofluid volume fraction is plotted in Figure
281 8. This figure shows that the viscosity enhancement due to the presence of nanotubes is

282 mainly evidenced for nanoparticles volume fraction of 0.055% and that the viscosity of
283 nanofluid is 6 times higher than the viscosity of the base fluid for nanoparticles volume
284 fraction of 0.55%. The influence of volume fraction on the enhancement of relative viscosity
285 of nanofluids is investigated in the following section, considering first the shape of the
286 nanotubes and then the presence of agglomerates network.

287

288 **4.3 Viscosity models: prediction and comparison with experimental data**

289

290 Some theoretical formulas have been developed to relate the relative viscosity of non-
291 aggregating colloidal suspensions or nanofluids to particle volume fraction. They are derived
292 from the pioneering model of Einstein [29]. This model is based on the assumption of viscous
293 fluid containing non-interacting hard spheres under particle volume fraction less than 1%.

294

$$295 \quad \mu_r = (1 + 2.5\phi) \quad (1)$$

296

297 where μ_r is the relative viscosity as defined by the ratio of the viscosity of the nanofluid μ_n to
298 the viscosity of the base fluid μ_{bf} , and ϕ is the volume fraction of nanoparticle in base fluid.
299 Later, Einstein's equation was extended by Brinkman [30] to suspensions with moderate
300 particle volume fraction, typically less than 4%.

$$301 \quad \mu_r = \frac{1}{(1 - \phi)^{2.5}} \quad (2)$$

302

303 Considering the Brownian motion of nanoparticles and the interaction between a pair of
304 particles, Batchelor [31] proposed the following equation.

305

$$306 \quad \mu_r = (1 + \eta\phi + k_H\phi^2 + \dots) \quad (3)$$

307

308 In equation (3), η is the intrinsic viscosity and k_H is the Huggins' coefficient. The values of η
309 and k_H are 2.5 and 6.5, respectively, for spherical particles.

310

311 For higher particle volume fraction, the Krieger-Dougherty relationship is considered as an
312 efficient model to relate the viscosity of non-aggregating colloidal suspensions or nanofluids
313 to particle volume fraction. This relationship is written as follows [32]:

314

315

$$\mu_r = \left(1 - \frac{\phi}{\phi_m}\right)^{-\eta\phi_m} \quad (4)$$

316

317 where η is the Einstein coefficient, $\eta=2.5$, and ϕ_m is the particle volume fraction when the
318 viscosity is infinite, defined as the maximum volume fraction. Typically, $\phi_m \approx 0.65$ for
319 random packing of hard spheres.

320 An equation with the same functional form was derived by Maron and Pierce from
321 consideration of the Ree-Eyring flow equations [33,34]. Noting that equation 5 was obtained
322 from a minimum principle applied to the energy dissipated by viscous effects.

323

324

$$\mu_r = \left(1 - \frac{\phi}{\phi_m}\right)^{-2} \quad (5)$$

325

326 The previous two equations reduce to the Einstein and Batchelor equations at first and second
327 order, respectively. The Maron-Pierce equation can also be used to predict the relative
328 viscosity of fiber suspensions, the maximum volume fraction ϕ_m depending also on the aspect
329 ratio of the fibers [35]. So, the value of the maximum volume fraction decreases with
330 increasing aspect ratio. A value of $\phi_m \approx 0.0361$ is here obtained due to the aspect ratio of the
331 nanotubes used [35]. This is very low in comparison of the maximum volume fraction of
332 spheres, thus showing the effect of nanoparticle shape.

333 As mentioned before, many nanoparticles have a non-spherical shape. So Brenner and
334 Condiff [36] have also developed a viscosity model to consider the shape effects in dilute
335 suspension. So, for rod-like particles, the Brenner-Condiff equation is applicable for a volume
336 fraction up to $1/r^2$ (this corresponds here to 0.004% in volume) and for viscosity at high shear
337 rate, where r is the aspect ratio of nanoparticles.

338

339

$$\mu_r = (1 + \eta\phi) \quad (6)$$

340

341 with

342

343

$$\eta = \frac{0.312r}{\ln 2r - 1.5} + 2 - \frac{0.5}{\ln 2r - 1.5} - \frac{1.872}{r} \quad (7)$$

344

345

346 In the presence of agglomerates, it was reported that the relative viscosity of aggregating
 347 suspensions or nanofluids can be modelled from the application of the fractal concept [37].
 348 So, the geometry of the aggregates can be described as a fractal like structure with a fractal
 349 index D. Assuming that the aggregates density change with the radial position and is not
 350 uniform in the nanofluid [8], the effective volume fraction of nanoparticles, denoted ϕ_a , is
 351 written as follows

$$\phi_a = \phi \left(\frac{a_a}{a} \right)^{3-D} \quad (8)$$

354 where a_a and a are the aggregates and primary nanoparticles radii respectively.

355 This leads to the modified Krieger-Dougherty formula given by equation (9) which was
 356 successfully applied to model the viscosity enhancement of aggregating nanofluids made of
 357 spherical particles [11,38] and rod-like particles [8,9,39].

$$\mu_r = \left(1 - \frac{\phi_a}{\phi_m} \right)^{-\eta\phi_m} \quad (9)$$

362 As a consequence, the modified Maron-Pierce equation can also be written [40]:

$$\mu_r = \left(1 - \frac{\phi_a}{\phi_m} \right)^{-2} \quad (10)$$

366 As previously reported [8], the fractal index D can depend on the type of aggregation, particle
 367 size and shape and shear flow condition. So, for aggregating nanofluids with spherical
 368 particles, D has been reported to be between 1.6 and 2.3 [41-43]. However, a value of 1.8 is
 369 typically used [40,44]. For aggregating nanofluids with nanorods or nanotubes, D varies
 370 between 1.5 and 2.45 as reported by [39]. Mohraz et al. [45] showed that the fractal index
 371 depends on the aspect ratio of nanorods. They reported that D increases from 1.8 to 2.3 for r
 372 ranging from 1 to 30.6 respectively. A value of 2.1 is generally taken [8,45,46]. Such a value
 373 was also obtained by Chatterjee and Krishnamoorti [47] for single walled carbon nanotubes
 374 (SWCNTs) dispersed in PEO, and by Khalkhal and Carreau [48] for MWCNTs dispersed in

376 epoxy resin, and a value of 2.05 was reported by Chen et al. [49] for SWCNTs dispersed in
377 aqueous suspensions. Based on the above, a value of 2.1 was taken for the fractal index in the
378 present work.

379 Comparison of the experimental data with the predicted data from the above formulas is
380 shown in figure 8. It is clear that the Einstein, Brinkman, Brenner and Condiff and Maron-
381 Pierce formulas cannot predict the relative viscosities of the CNT water based nanofluids for
382 volume concentration exceeding 0.027%. In addition, the difference between the experimental
383 and the computed values increases with the volume fraction. This result shows the strong
384 influence of agglomerates which significantly increase the effective volume of the nanotubes
385 and thus the relative viscosity of the nanofluid. This also confirms the conclusions reported
386 previously from the steady state apparent viscosity curves.

387 Nevertheless, figure 8 shows excellent agreement between the prediction of the modified
388 model of Maron-Pierce and experimental data when $a_a/a \approx 4.41$, as the average deviation of
389 experimental relative viscosity compared to the model is less than 5%. If a is taken as the
390 average length of the nanotubes, this leads to a maximum aggregates size close to 6.6 nm,
391 which is in quite good agreement with the maximum size of CNT aggregates determined from
392 SEM analyses [25]. A comparison of our results with the data of Chen et al. [38] (EG-
393 spherical TiO_2 , $d=25\text{nm}$, $a_a/a=3.34$, $D=1.8$, $\phi_m=0.605$), the data of Kole and Dey [11] (gear oil-
394 spherical CuO , $d=40\text{nm}$, $a_a/a=7.15$, $D=1.7$, $\phi_m=0.605$) and the data of Chen et al. [8] (EG-
395 TNT, $r \approx 10$, $a_a/a=9.46$, $D=2.1$, $\phi_m=0.3$), suggests that the size and the aspect ratio are an
396 important factor in the formation of nanoclusters within the nanofluids in spite of the use of
397 surfactant. This shows the influence of particle length on the entanglement of the
398 nanoparticles, the presence and the size of agglomerates.

399

400 **5. Conclusion**

401 We have presented an experimental investigation of the rheological properties of water-based
402 nanofluids containing carbon nanotubes (CNT) with large aspect ratio. The influence of
403 particle concentration and temperature on the viscosity of the nanofluids was discussed and
404 the nanofluids were shown to behave as a shear-thinning material at high particle content. For
405 lower particle content, the nanofluids behave in Newtonian manner. It was also reported that
406 temperature affects the viscosity of nanofluids and base fluids but that the relative viscosity of
407 nanofluids at high shear rate is independent of temperature. The relative viscosity of
408 nanofluids at high shear rate is strongly enhanced with their particle content showing the

409 presence of aggregates, and can be modelled by the Maron-Pierce equation considering the
410 influence of nanoparticles agglomerates. An average maximum size of aggregates was thus
411 evaluated and favourably compared with SEM characterization previously done. The results
412 of this experimental study also show the relevance of the rheological characterization
413 concerning the presence and the structural information of nanofluids aggregates and can
414 contribute to the understanding of the thermal properties of such materials.

415

416

417 **Acknowledgments**

418

419 Nanocycl Belgium is gratefully acknowledged for providing the CNT water based nanofluid.

420

421 **References**

422

423 [1] D.S. Wen, Y.L. Ding, Effective thermal conductivity of aqueous suspensions of carbon
424 nanotubes (nanofluids), *J. Thermophys. Heat Transfer* 18 (2004) 481-485.

425

426 [2] M.J. Assael, I.N. Mataxa, J. Arvanitidis, D. Christophilos, C. Lioutas, Thermal
427 conductivity enhancement in aqueous suspensions of carbon multi-walled and double-walled
428 nanotubes in the presence of two different dispersants, *Int. J. Thermophys.* 26 (2005) 647-
429 664.

430

431 [3] X.Q. Wang, A.S. Mujumdar, Heat transfer characteristics of nanofluids: A review, *Int. J.*
432 *Therm. Sci.* 46 (2007) 1-19.

433

434 [4] S.M.S. Murshed, K.C. Leong, C. Yang, Investigations of thermal conductivity and
435 viscosity of nanofluids, *Int. J. Therm. Sci.* 47 (2008) 560-568.

436

437 [5] D. Wen, S. Lin, S. Vafaei, K. Zhang, Review of nanofluids for heat transfer applications,
438 *Particuology* 7 (2009) 141-150.

439

440 [6] D. Wu, H. Zhu, L. Wang, L. Liua, Critical issues in nanofluids preparation,
441 characterization and thermal conductivity, *Curr. Nanosci.* 5 (2009) 103-112.

442

443 [7] H. Chen, W. Yang, Y. He, Y. Ding, L. Zhang, C. Tan, A.A. Lapkin, D.V.Bavykin, Heat
444 transfer and flow behaviour of aqueous suspensions of titanate nanotubes (nanofluids),
445 *Powder Tech* 183 (2008) 63-12.

446

447 [8] H. Chen, Y. Ding, A.A. Lapkin, X. Fan, Rheological behaviour of ethylene glycol-titanate
448 nanotube nanofluid, *J. Nanopart. Res.* 11 (2009) 1513-1520.

449

450 [9] H. Chen, Y. Ding, A.A. Lapkin, Rheological behaviour of nanofluids containing tube/rod-
451 like nanoparticles, *Powder Tech.* 194 (2009) 132-141.

452

- 453 [10] S.Q. Zhou, R. Ni, D. Funfschilling, Effects of shear rate and temperature on viscosity of
454 alumina polyalphaolefins nanofluids, *J. Appl. Phys.* 107 (2010) 054317.
455
- 456 [11] M. Kole, T.K. Dey, Effect of aggregation on the viscosity of copper oxide-gear oil
457 nanofluids, *Int. J. Thermal Sci.* 50 (2011) 1741-1747.
458
- 459 [12] P.J. Harris, Carbon nanotubes and related structures: new materials for the 21st century,
460 Cambridge, University Press, 1999.
461
- 462 [13] Y. Otsubo, M. Fujiwara, M. Kouno, K. Edamura, Shear-thickening flow of suspensions
463 of carbon nanofibers in aqueous PVA solutions, *Rheol. Acta* 46 (2007) 905-912.
464
- 465 [14] M.F. Yu, B.S. Files, S. Arepalli, R.S. Ruoff, Tensile loading of ropes of single wall carbon
466 nanotubes and their mechanical properties, *Physical Rev Lett* 84 (2000) 5552-5.
467
- 468 [15] L. Vaisman, H.D. Wagner, G. Marom, The role of surfactants in dispersion of carbon
469 nanotubes, *Adv. Coll. Int. Sci.* 128-130 (2006) 37-46.
470
- 471 [16] L. Chen, H. Xie, W. Yu, Nanofluids containing carbon nanotubes treated by
472 mechanochemical reaction, *Thermoch. Acta* 477 (2008) 21-24.
473
- 474 [17] H. Wang, Dispersing carbon nanotubes using surfactants, *Curr. Opinion Coll. Interface*
475 *Sci.* 14 (2009) 364-371.
476
- 477 [18] A. Nasiri, M. Shariaty-Niasar, A. Rashidi, A. Amrollahi, R. Khodafarin, Effect of
478 dispersion method on thermal conductivity and stability of nanofluid, *Exp. Thermal Fluid Sci.*
479 35 (2011) 717-723.
480
- 481 [19] T.X. Phuoc, M. Massoudi, R.H. Chen, Viscosity and thermal conductivity of nanofluids
482 containing carbon nanotubes stabilized by chitosan, *Int. J. Thermal Sci.* 50 (2011) 12-18.
483
- 484 [20] P. Garg, L.A. Jorge, C. Marsh, T.A. Carlson, D.A. Kessler, K. Annamalai, An
485 experimental study on the effect of ultrasonication on viscosity and heat transfer performance
486 of multi-wall carbon nanotube-based aqueous nanofluids, *Int. J. Heat Mass Transfer* 52 (2009)
487 5090–5101.
488
- 489 [21] Y. Yang, E.A. Grulke, Z.G. Zhanh, G. Wu, Thermal and rheological properties of carbon
490 nanotube-in-oil dispersions, *J. Appl. Phys.* 99 (2006) 114307.
491
- 492 [22] S. Kanagaraj, F.R. Varabda, A. Fonseca, J. Ponmozhi, J.A. Lopez da Silva, M.S.A.
493 Oliveira et al, Rheological study of nanofluids at different concentration of carbon nanotubes,
494 19th National & 8th ISHMT-ASME Heat Mass Transfer Conf., January 3-5, 2008 hvderabad,
495 India (paper NFF-7).
496
- 497 [23] J. Ponmozhi, F.A.M.M. Gonçalves, A.G.M. Feirreira, I.M.A Fonseca , S. Kanagaraj, M.
498 Martins, M.S.A. Oliveira, Thermodynamic and transport properties of CNT water based
499 nanofluids, *J. Nano Res.* 11 (2010) 101-106.
500

- 501 [24] B. Aladag, S. Halelfadl, N. Doner, T. Maré, S. Duret, P. Estellé, Experimental
502 investigations of the viscosity of nanofluids at low temperatures, *App. Energy*, 97 (2012)
503 876-880.
504
- 505 [25] P. Estellé, S. Halelfadl, N. Doner, T. Maré, Shear flow history effect on the viscosity of
506 carbon nanotubes water based nanofluid, *Current Nanoscience*, 9/2 (2013) 225-230.
507
- 508 [26] L. Chen, H. Xie, W. Yu, Y. Li, The rheological behaviors of nanofluids containing multi-
509 walled carbon nanotube, *J. Disp. Sci. Tech.* 32 (2011) 550-554.
510
- 511 [27] Y. Ding, H. Alias, D. Wen, R.A. Williams, Heat transfer of aqueous suspensions of
512 carbon nanotubes (CNT nanofluids), *Int. J. Heat Mass Transfer* 49 (2006) 240-250.
513
- 514 [28] T. Maré, S. Halelfadl, O. Sow, P. Estellé, S. Duret, F. Bazantay, Comparison of the
515 thermal performances of two nanofluids at low temperature in a plate heat exchanger, *Exp.*
516 *Thermal Fluid Sci* 35 (2011) 1535-1543.
517
- 518 [29] A. Einstein, *Investigations on the Theory of the Brownian Movement*, Dover
519 Publications, Inc., New York, 1956.
520
- 521 [30] H.C. Brinkman, The viscosity of concentrated suspensions and solutions, *J. Chem. Phys.*
522 20 (1952) 571-581.
523
- 524 [31] G. Batchelor, The effect of Brownian motion on the bulk stress in a suspension of
525 spherical particles, *J. Fluid Mech.* 83 (1977) 97-117.
526
- 527 [32] I.M. Krieger, T.J. Dougherty, A mechanism for non-Newtonian flow in suspension of
528 rigid spheres, *J. Trans. Soc. Rheol.* 3 (1959) 137-152.
529
- 530 [33] S.H. Maron, P.E. Pierce, Application of Ree-Eyring generalized flow theory to
531 suspensions of spherical particles, *J. Colloid Sci.* 11 (1956) 80-95.
532
- 533 [34] M.M. Cross, Viscosity-concentration-shear rate relations for suspensions, *Rheol. Acta* 14
534 (1975) 402-403.
535
- 536 [35] S. Mueller, E.W. Llewellyn, H.M. Mader, The rheology of suspensions of solid particles.
537 *Proc. of The Royal Society A*, 466 (2010) 1201-1228.
538
- 539 [36] H. Brenner, D.W. Condiff, Transport mechanics in systems of orientable particles. Part
540 IV. Convective transport, *J. Colloid Int. Sci.* 47 (1974) 199-264.
541
- 542 [37] W. Wolthers, M.H.G. Duits, D. van den Ende, J. Mellema, Shear history dependence of
543 aggregated colloidal dispersions, *J. Rheol.* 40 (1996) 799-811.
544
- 545 [38] H. Chen, Y. Ding, C. Tan, Rheological behavior of nanofluids, *New J. Phys.* 9 (2007)
546 367.
547
- 548 [39] H. Chen, S. Witharana, Y. Jin, C. Kim, Y. Ding, Predicting thermal conductivity of
549 liquids suspensions of nanoparticles (nanofluids) based on rheology, *Particuology* 7 (2009)
550 151-157.

551
552 [40] J. Chevalier, O. Tillement, F. Ayela, Structure and rheology of SiO₂ nanoparticle
553 suspensions under very high shear rates, *Phys Rev E* 80 (2009) 051403.
554
555 [41] T.D. Waite, J.K. Cleaver, J.K. Beattie, Aggregation kinetics and fractal structure of
556 gamma-alumina assemblages, *J. Colloid Int. Sci.* 241 (2001) 333–339.
557
558 [42] B.X. Wang, L.P. Zhou, X.F. Peng, A fractal model for predicting the effective thermal
559 conductivity of liquid with suspension of nanoparticles, *Int. J. Heat Mass Transf.* 46 (2003)
560 2665–2672.
561
562 [43] Y. Xuan, Q. Li, W. Hu, Aggregation structure and thermal conductivity of nanofluids,
563 *AIChE J.* 49 (2003) 1038–1043.
564
565 [44] R. Prasher, P.E. Phelan, P. Bhattacharya, Effect of aggregation kinetics on the thermal
566 conductivity of nanoscale colloidal solutions (nanofluid), *Nano Lett.* 6 (2006) 1529.
567
568 [45] A. Mohraz, D.B. Moler, R.M. Ziff, M.J. Solomon, Effect of monomer geometry on the
569 fractal structure of colloidal rod aggregates, *Phys. Rev. Lett.* 92 (2004) 155503.
570
571 [46] J.M. Lin, T.L. Lin, U. Jeng, Y. Zhong, C. Yeh, T. Chen, Fractal aggregates of the Pt
572 nanoparticles synthesized by the polyol process and poly(N-vinyl-2-pyrrolidone) reduction, *J.*
573 *Appl. Crystallogr.* 40 (2007) 540-543.
574
575 [47] T. Chatterjee, R. Krishnamoorti, Dynamic consequences of the fractal network of
576 nanotube-poly(ethylene oxide) nanocomposites, *Phys. Rev. E Stat. Nonlinear Soft Matter*
577 *Phys.* 75 (2007) 050403.
578
579 [48] F. Khalkhal, P.J. Carreau, Scaling behavior of the elastic properties of non-dilute
580 MWCNT-epoxy resin, *Rheol. Acta* 50 (2011) 717-728.
581
582 [49] Q. Chen, C. Saltiel, S. Manickavasagam, L.S. Schadler, R.W. Siegel, H. Yang ,
583 Aggregation behavior of single-walled carbon nanotubes in dilute aqueous suspension, *J.*
584 *Colloid Interface Sci.* 280 (2004) 91-97.
585

586 **Figure Captions**

587

588 Figure 1. SEM image taken from dried starting nanofluid [25] (This figure was reprinted with
589 the permission of Bentham Science Publishers)

590

591 Figure 2. Apparent shear viscosity of the base fluid corresponding to the nanofluid with
592 0.55% in CNT volume fraction – Influence of temperature.

593

594 Figure 3. Apparent shear viscosity of the base fluid corresponding to the nanofluid with
595 0.0055% in CNT volume fraction– Influence of temperature.

596

597 Figure 4. Apparent shear viscosity of nanofluid with 0.278% in CNT volume fraction –
598 Influence of temperature.

599

600 Figure 5. Apparent shear viscosity of nanofluid with 0.0055% in CNT volume fraction –
601 Influence of temperature.

602

603 Figure 6. Viscosity of nanofluids at 20°C as a function of shear rate for different volume
604 fraction of nanotubes.

605

606 Figure 7. Relative viscosity of nanofluids as a function of particle volume content and
607 temperature.

608

609 Figure 8. Relative viscosity of nanofluids as a function of particle volume content and
610 temperature - Comparison of experimental data and viscosity models.

611

612

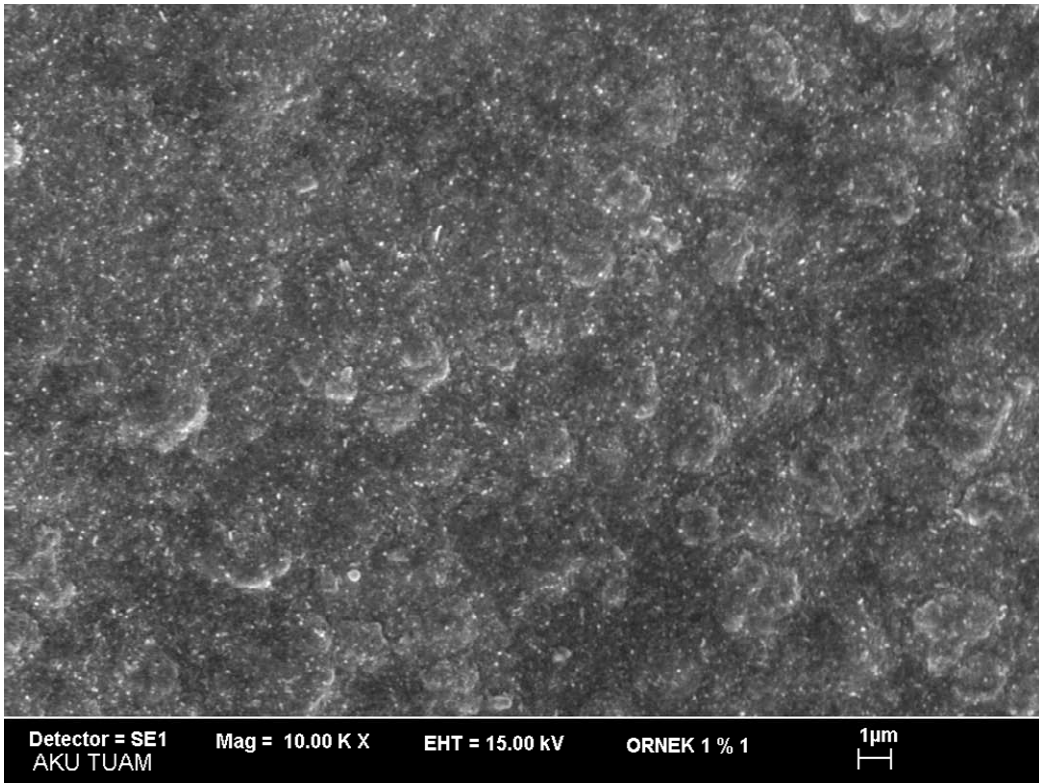
613 **Table Caption**

614

615 Table 1. Volume fraction of tested nanofluids and corresponding base fluids, and shear
616 viscosity of base fluids as a function of SDBS volume fraction and temperatures.

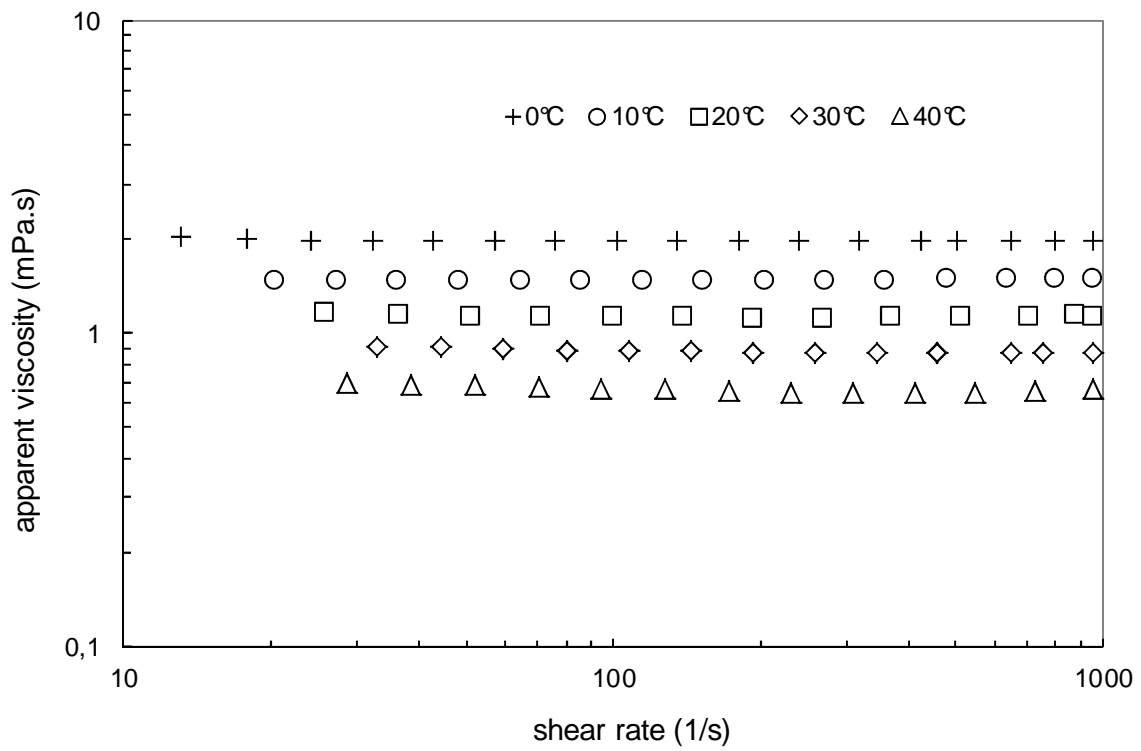
617

618



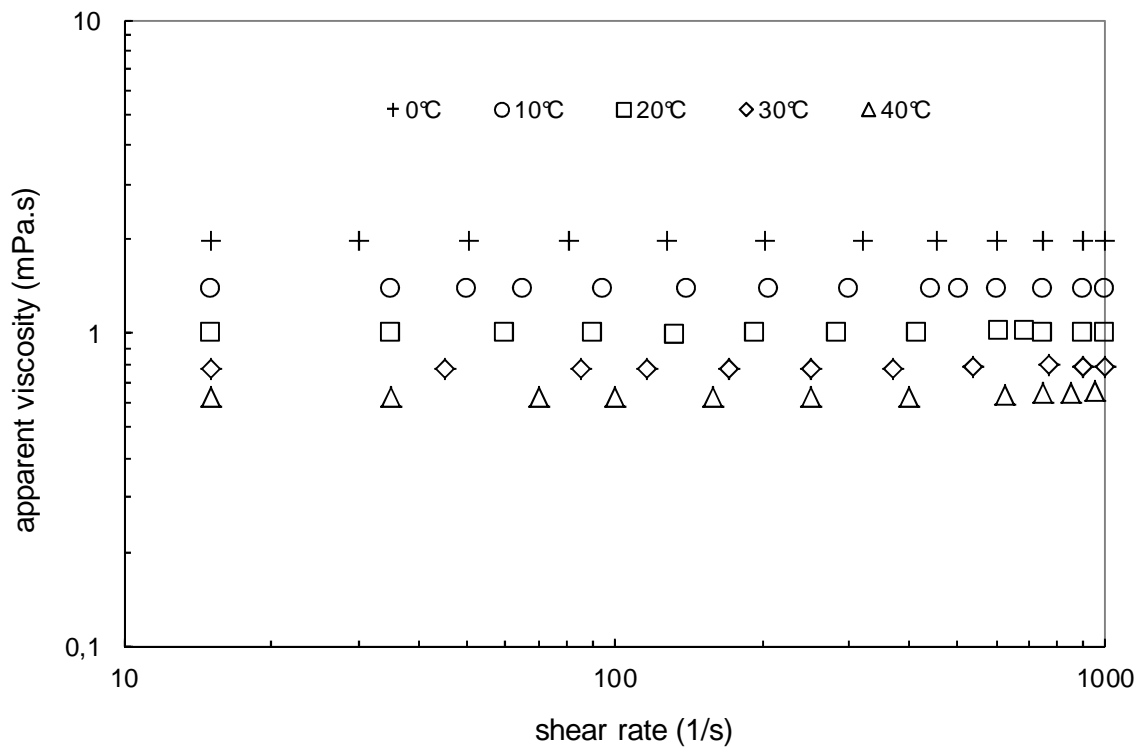
619
620
621
622
623
624
625

Figure 1. SEM image taken from dried starting nanofluid [25] (This figure was reprinted with the permission of Bentham Science Publishers)

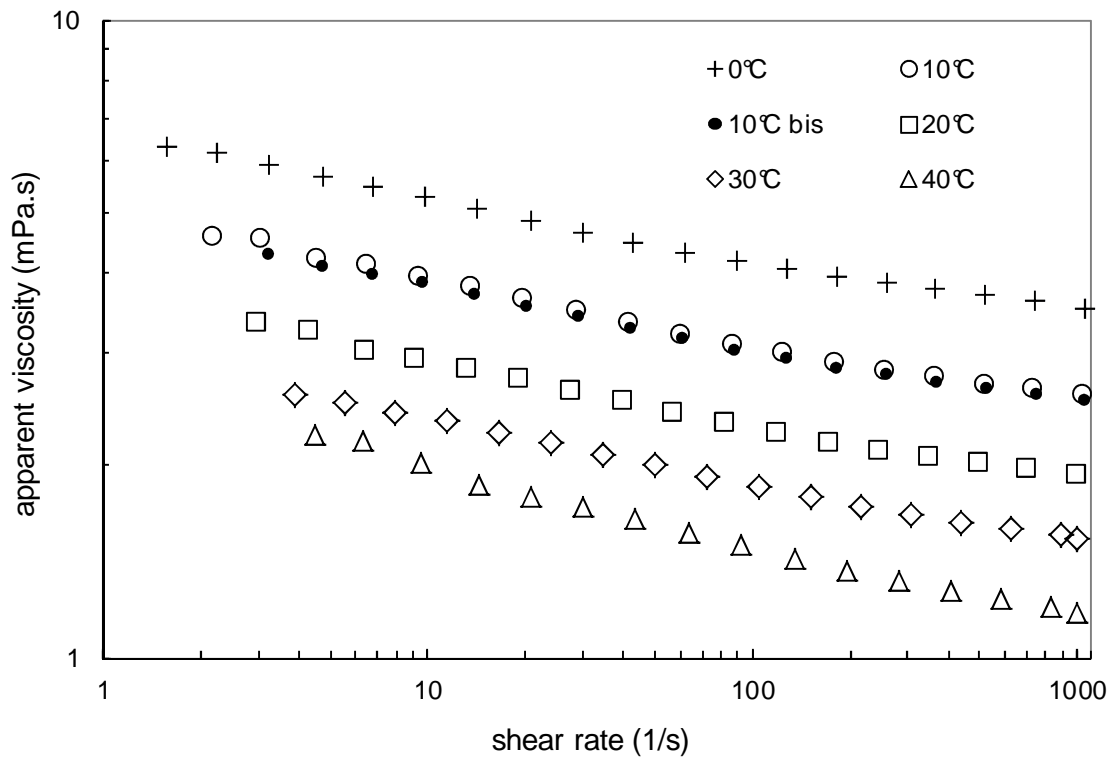


627
628
629
630

Figure 2. Apparent shear viscosity of the base fluid corresponding to the nanofluid with 0.55% in volume fraction – Influence of temperature.

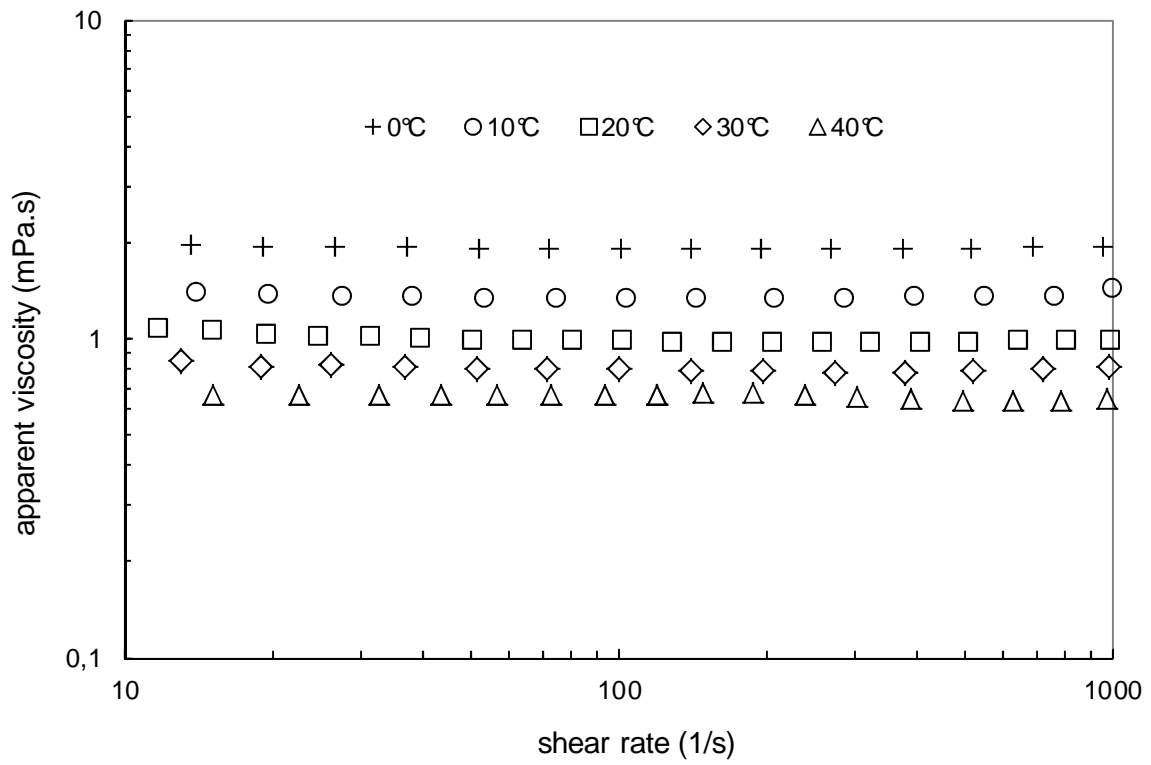


632 Figure 3. Apparent shear viscosity of the base fluid corresponding to the nanofluid with
 633 0.0055% in volume fraction– Influence of temperature.
 634
 635
 636

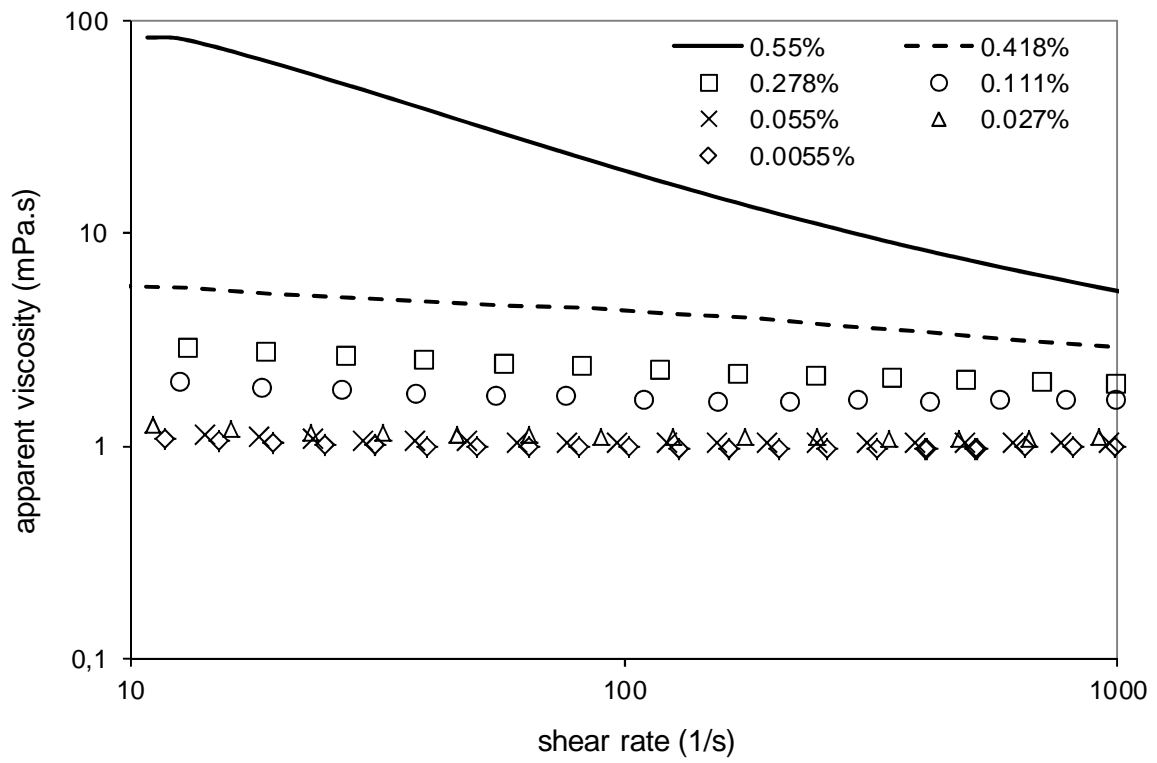


638
 639
 640
 641

Figure 4. Apparent shear viscosity of nanofluid with 0.278% in CNT volume fraction – Influence of temperature.

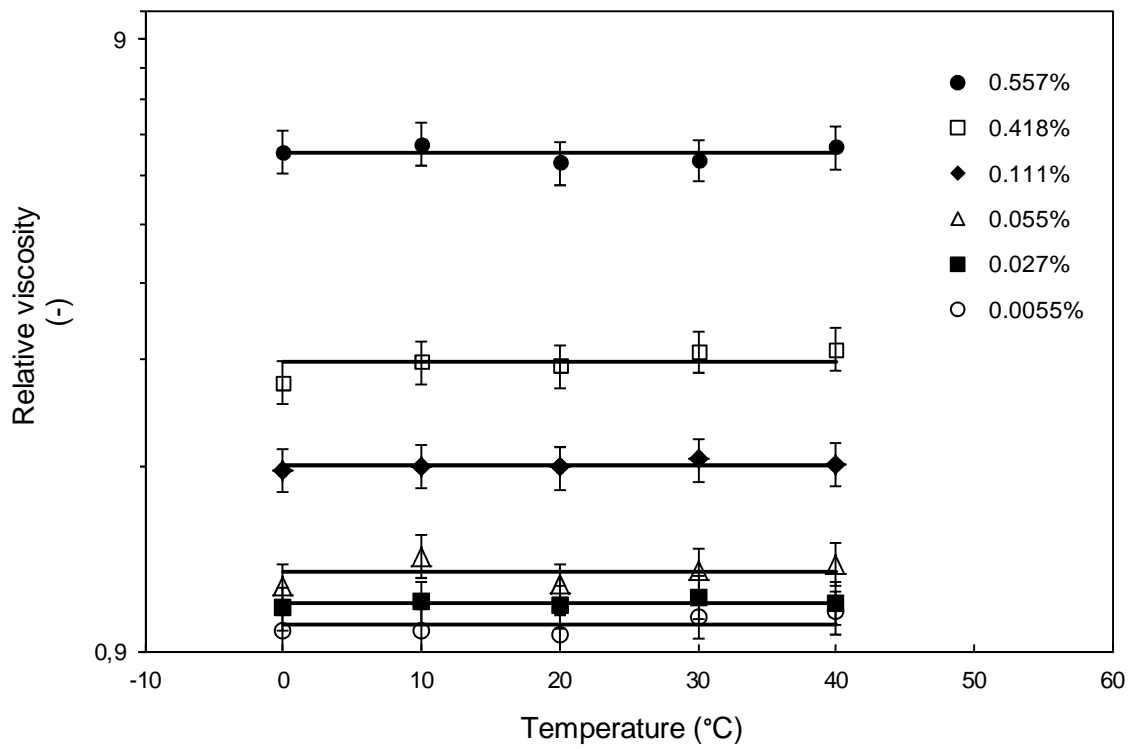


643
644 Figure 5. Apparent shear viscosity of nanofluid with 0.0055% in CNT volume fraction –
645 Influence of temperature.
646



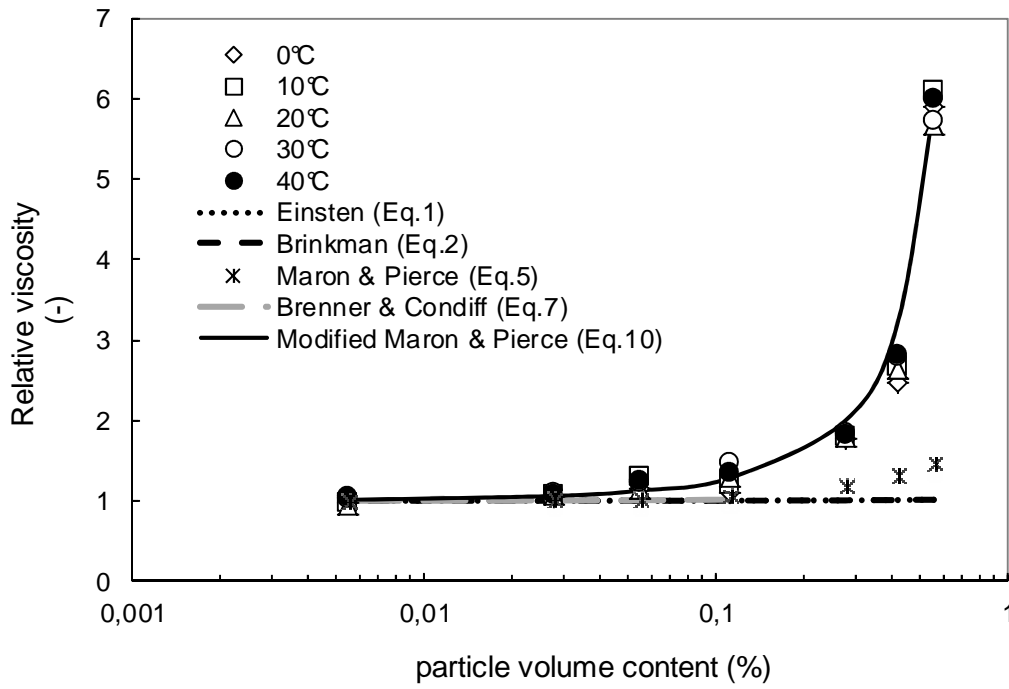
648
 649
 650
 651

Figure 6. Viscosity of nanofluids at 20°C as a function of shear rate for different volume fraction of nanotubes.



652
 653
 654
 655

Figure 7. Relative viscosity of nanofluids as a function of particle volume content and temperature.



657
 658
 659
 660

Figure 8. Relative viscosity of nanofluids as a function of particle volume content and temperature - Comparison of experimental data and viscosity models.

661 Table 1. Volume fraction of tested nanofluids and corresponding base fluids, and shear
 662 viscosity of base fluids as a function of SDBS volume fraction and temperatures.
 663

Volume fraction (%)		Shear viscosity of base fluids (mPa.s)				
CNT	SDBS	0 (°C)	10 (°C)	20 (°C)	30 (°C)	40 (°C)
0.557	1.697	1.98	1.478	1.129	0.877	0.665
0.418	1.272	1.975	1.454	1.102	0.852	0.657
0.278	0.847	1.97	1.401	1.077	0.828	0.648
0.111	0.338	1.964	1.391	1.046	0.799	0.637
0.055	0.169	1.962	1.386	1.036	0.789	0.633
0.0277	0.084	1.961	1.383	1.027	0.784	0.632
0.0055	0.0169	1.96	1.382	1.026	0.780	0.630

664